



Carbonate saturation state of surface waters in the Ross Sea and Southern Ocean: controls and implications for the onset of aragonite undersaturation

H. B. DeJong, R. B. Dunbar, D. Mucciarone, and D. A. Koweeck

Department of Earth System Science, Stanford University, Stanford, CA, USA

Correspondence to: H. B. DeJong (hdejong@stanford.edu)

Received: 6 May 2015 – Published in Biogeosciences Discuss.: 8 June 2015

Revised: 30 October 2015 – Accepted: 23 November 2015 – Published: 2 December 2015

Abstract. Predicting when surface waters of the Ross Sea and Southern Ocean will become undersaturated with respect to biogenic carbonate minerals is challenging in part due to the lack of baseline high-resolution carbon system data. Here we present ~ 1700 surface total alkalinity measurements from the Ross Sea and along a transect between the Ross Sea and southern Chile from the austral autumn (February–March 2013). We calculate the saturation state of aragonite (Ω_{Ar}) and calcite (Ω_{Ca}) using measured total alkalinity and pCO_2 . In the Ross Sea and south of the Polar Front, variability in carbonate saturation state (Ω) is mainly driven by algal photosynthesis. Freshwater dilution and calcification have minimal influence on Ω variability. We estimate an early spring surface water Ω_{Ar} value of ~ 1.2 for the Ross Sea using a total alkalinity–salinity relationship and historical pCO_2 measurements. Our results suggest that the Ross Sea is not likely to become undersaturated with respect to aragonite until the year 2070.

to preindustrial levels (Caldeira and Wickett, 2003; Archer et al., 2009).

The saturation state (Ω) of seawater with respect to a specific calcium carbonate ($CaCO_3$) mineral (aragonite, calcite, or magnesium calcite) is defined as

$$\Omega = \frac{[Ca^{2+}][CO_3^{2-}]}{K_{sp}}, \quad (1)$$

where K_{sp} is the solubility product constant for the specific $CaCO_3$ mineral and depends on salinity, temperature, and pressure (Mucci, 1983). Aragonite is ~ 1.6 times more soluble than calcite at $0^\circ C$ whereas the solubility of magnesium calcite varies depending on the mole fraction of magnesium ions (Dickson, 2010). Ω_{Ar} represents the saturation state of aragonite and Ω_{Ca} represents the saturation state of calcite. $\Omega < 1$ represents undersaturation where dissolution is thermodynamically favorable and $\Omega > 1$ represents supersaturation where precipitation is favorable. Most surface waters of the global oceans are currently supersaturated with respect to $CaCO_3$ (Feely et al., 2009). However, for some species including coccolithophorids, foraminifera, and tropical corals, decreasing CO_3^{2-} concentrations can decrease calcification rates even in supersaturated conditions (Riebesell et al., 2000; Moy et al, 2009; Andersson et al., 2011).

The Southern Ocean is especially vulnerable to ocean acidification (OA) due to its relatively low total alkalinity (TA) and because of increased CO_2 solubility in cold water. In addition, Antarctic continental shelves have insignificant sedimentary $CaCO_3$ to buffer against OA (Hauck et al., 2013). Modeling studies predict that surface waters in the Southern Ocean may start to become undersaturated with

1 Introduction

Atmospheric CO_2 concentrations have increased by 40 % since preindustrial times to ~ 400 ppm today and could reach 936 ppm by the year 2100 (IPCC AR5 WG1, 2013). Due to oceanic uptake of CO_2 , surface ocean pH is already 0.1 units lower than preindustrial values and is projected to decrease by another 0.3–0.4 units by the end of the century, equivalent to a 50 % decrease in carbonate ion (CO_3^{2-}) concentrations (Orr et al., 2005). Even after CO_2 emissions are halted, it will take thousands of years before the surface ocean pH returns

respect to aragonite by 2050 and be fully undersaturated by 2100 (Orr et al., 2005; Feely et al., 2009). McNeil and Matear (2008) have suggested that wintertime aragonite undersaturation in the Southern Ocean may begin as early as 2030.

OA-induced decreases in Ω have potentially serious consequences for Antarctic food webs. In the Ross Sea the aragonitic shelled pteropod *Limacina helicina* is a dominant zooplankton that can reach densities of 300 individuals m^{-3} (Hopkins, 1987; Seibel and Dierssen, 2003; Hunt et al., 2008). Pteropods are important prey for notothenioid fish, which in turn are major prey for penguins, seals, and whales (Foster and Montgomery, 1992; La Mesa et al., 2000, 2004). Pteropods may also be important contributors to the biological pump (Collier et al., 2000; Accornero et al., 2003; Manno et al., 2010). Orr et al. (2005) found that the shell of a subarctic pteropod started to dissolve within 48 h when placed in waters with the level of aragonite saturation expected to occur in the Southern Ocean by 2100. Severe dissolution pitting was observed on live pteropods that were collected from the upper 200 meters in the Atlantic sector of the Southern Ocean, from waters that were near undersaturation with respect to aragonite (Bednaršek et al., 2012).

Other organisms in the Southern Ocean may be negatively impacted by OA include krill (Kawaguchi et al., 2013), foraminifera (Moy et al., 2009), sea urchins (Sewell and Hofmann, 2011), deep sea hydrocorals (Shadwick et al., 2014), sea stars (Gonzalez-Bernat et al., 2013), bivalves (Cummings et al., 2011), and brittle stars (McClintock et al., 2011). Conversely non-calcareous phytoplankton may benefit in the Ross Sea in a high pCO_2 world, especially the larger diatom *Chaetoceros lineola* (Tortell et al., 2008; Feng et al., 2010).

There are only a few surface carbon system data sets from the Ross Sea (Bates et al., 1998; Sweeney et al., 2000b; Sandrini et al., 2007; Long et al., 2011; Mattsdotter Björk et al., 2014; Rivaro et al., 2014; Kapsenberg et al., 2015) that can be used to establish baselines in order to understand the relative importance of physical, chemical, and biological processes that drive the large spatial and seasonal variability of Ω . With no winter Ω measurements, it is challenging to predict when the Ross Sea will become undersaturated with respect to aragonite and calcite. A model by McNeil et al. (2010) suggests that winter surface waters in the Ross Sea will become undersaturated with respect to aragonite by the year 2045 since sea ice, upwelling of deep water, and short residence times prevent these surface waters from reaching equilibrium with the atmosphere. However, McNeil et al. (2010) indirectly estimated surface winter Ω_{Ar} values by using limited carbon system data from the spring (Sweeney et al., 2000b).

We present ~ 1700 underway TA measurements from the surface waters of the Ross Sea and along a transect across the Southern Ocean from the Ross Sea to southern Chile. By combining the underway TA measurements with pCO_2 data we characterize the complete carbon system and describe patterns and controls on Ω variability. Finally, af-

ter establishing a relationship between salinity and TA, we use the Lamont Doherty Earth Observatory (LDEO) pCO_2 database (Takahashi et al., 2009) (available at <http://www.ldeo.columbia.edu/res/pi/CO2>) to provide an independent estimate of Ross Sea surface water Ω_{Ar} in early spring.

2 Study site

The Antarctic Circumpolar Current (ACC) flows from east to west around the entire Antarctic continent and is composed of multiple fronts that separate distinct water masses (Rintoul et al., 2001). There are three primary fronts – the southern ACC front (SACCF), the Antarctic Polar Front (PF), and the Subantarctic Front (SAF) (Orsi et al., 1995). Sokolov and Rintoul (2009) found that these primary fronts are composed of multiple jets that they label south (S), middle (M), and north (N). Convergent Ekman transport north of the westerly wind stress maximum (near the axis of the ACC) downwells surface water into the ocean interior. Circumpolar Deep Water (CDW) upwells south of the wind stress maximum where it becomes modified into Antarctic surface water (AASW) (Rintoul et al., 2001).

The cyclonic Ross Sea gyre is located south of the ACC (Smith et al., 2012). The southern portion of this gyre flows west along the Ross Sea continental slope and generates intrusions of CDW onto the Ross Shelf through the major troughs (Orsi et al., 2009; Dinniman et al., 2011; Kohut et al., 2013). In addition, AASW enters the Ross Sea in the east and flows westward along the Ross Ice Shelf (Orsi et al., 2009).

The Ross Sea is considered a biological hotspot supporting over 400 benthic species (Smith et al., 2012). During the winter the Ross Sea is mostly covered by sea ice, which begins to clear in November to form the largest polynya in Antarctica. There are two main phytoplankton blooms in the Ross Sea. The first bloom begins in late November in the Ross Sea polynya (Fig. 1a) and peaks in mid- to late December (Arrigo et al., 1999; Arrigo and van Dijken, 2004). In early January, sea ice melts in the western Ross Sea, lowering surface salinity and increasing stratification (Fig. 1b). As a result, a secondary diatom bloom forms in the west with productivity peaking in late January to early February (Arrigo et al., 1999; Arrigo and van Dijken, 2004) (Fig. 1c).

The Ross Sea phytoplankton blooms account for up to half of all primary production over the Antarctic continental shelf (Arrigo and McClain, 1994; Smith and Gordon, 1997; Arrigo and van Dijken, 2003). Photosynthesis reduces the concentration of nutrients and dissolved inorganic carbon (DIC) in the mixed layer, causing Ω to increase in surface waters (McNeil et al., 2010). Once the sea ice reforms during autumn and winter, remineralization of organic matter and deep convective mixing produces a relatively homogeneous water column, causing surface DIC concentrations to increase and Ω to decrease (Gordon et al., 2000; Sweeney et al., 2000b; Petty et al., 2014).

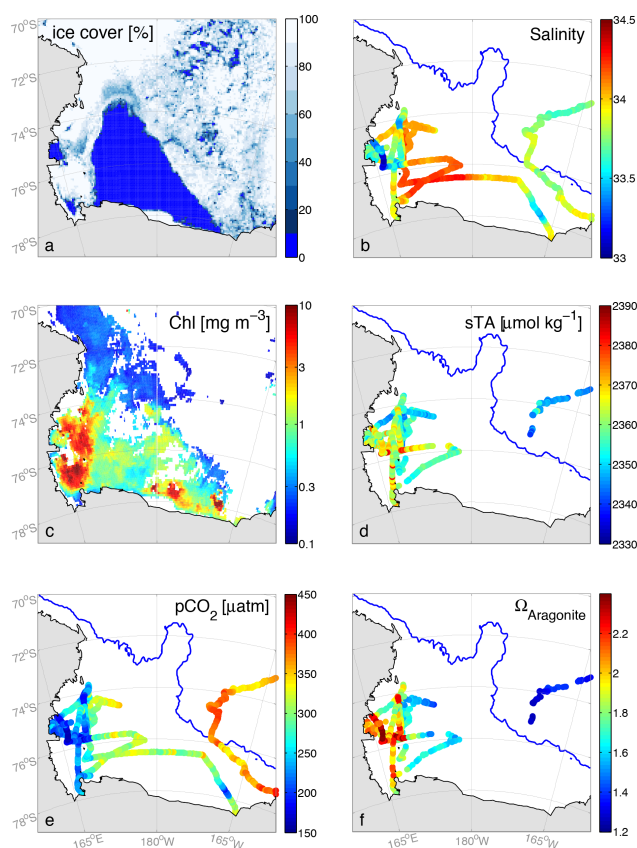


Figure 1. Maps of (a) 6.25 km gridded sea-ice concentration on 1 December 2012 from the University of Bremen, <http://www.iup.uni-bremen.de:8084/amsr2/> (Spreen et al., 2008); (b) sea surface salinity from NBP 13-02; (c) satellite chlorophyll concentration on February 2013 from the 9 km Level 3 Aqua MODIS product, <http://oceancolor.gsfc.nasa.gov/cgi/l3>; (d) sTA from NBP 13-02; (e) $p\text{CO}_2$ from NBP 13-02; (f) aragonite saturation state (Ω_{Ar}) from NBP 13-02.

3 Methods

3.1 Analytical methods

As part of the TRacing the fate of Algal Carbon Export in the Ross Sea (TRACERS) program, we undertook continuous measurements of surface water TA in the western Ross Sea aboard the *Nathaniel B. Palmer* (NBP13-02) from 13 February through 9 March 2013. In addition, from 19 March to 2 April 2013, we made continuous measurements of surface water TA in transit between the Ross Sea and southern Chile along the cruise track shown in Fig. 2. Underway TA measurements were conducted using the shipboard uncontaminated continuous flow system with an intake located at ~ 5 m depth. Seawater from the ship's underway system was redirected to the bottom of a 250 mL free surface interface cup flowing at 2 L min^{-1} and was drawn from the bottom of the cup for TA analysis without filtration. The entire system

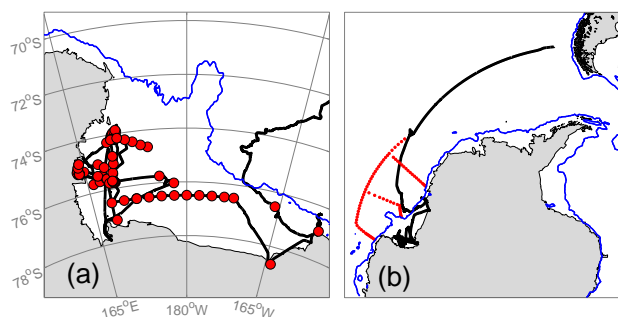


Figure 2. Cruise track (black line) from NBP 13-02. Stations used in this study (red circles) from (a) TRACERS (NBP 13-02) and (b) CLIVAR (NBP 11-02). Blue line is the 1000 m isobath.

was automated and relatively unattended. The sampling cycle was every 24 min on a custom-configured Metrohm 905 Titrand equipped with three Metrohm 800 Dosino syringe pumps (two 50 mL units for sample handling and rinsing and one 5 mL unit for acid titration). Temperature was measured at the cup and in the titration cell. We used certified 0.1 N HCl provided by A. Dickson (Scripps Institution of Oceanography) for the potentiometric titrations and TA calculations follow Dickson et al. (2003). Since we consumed the certified HCl after ~ 1000 measurements in the Ross Sea, we have no TA data from the eastern Ross Sea. For the transect to southern Chile, we mixed our own 0.1 N HCl solution (from 12.1 N HCl, laboratory grade NaCl, and deionized water). We calibrated TA measurements using certified reference materials (CRMs) Batch 122 provided by A. Dickson (Scripps Institution of Oceanography). Our estimated precision for the underway TA measurements from 68 CRM analyses is $\pm 3 \mu\text{mol kg}^{-1}$ (± 1 SD).

Outlier TA analyses were identified by taking a running mean and standard deviation of nine consecutive measurements. A measurement was rejected if (1) the difference between the measurement and mean was greater than twice the standard deviation and (2) the difference between the measurement and mean was greater than $6 \mu\text{mol kg}^{-1}$. A total of 65 measurements (out of 1716) were rejected.

We collected seawater samples for particulate organic carbon (POC) every 2 h from the ship's continuous flow system between the Ross Sea and Chile. Following the protocols of Knap et al. (1996), we filtered 1 to 3 L of seawater through precombusted Whatman GFC filters and immediately rinsed these filters with 10 mL of 0.01 N HCl to remove carbonate. We air-dried the filters before sending them to Stanford University where they were analyzed on a Carlo Erba NA1500 Series 2 elemental analyzer.

Surface $p\text{CO}_2$ measurements were made every 3 min using the LDEO air–sea equilibrator permanently installed on the NBP (data available at <http://www.ldeo.columbia.edu/res/pi/CO2>). The estimated precision is $\pm 1.5 \mu\text{atm}$.

Underway salinity and sea surface temperature (SST) were measured continuously by the ship's thermosalinograph (TSG) (Sea-Bird model SBE-45). These variables were binned into 1 min intervals.

We collected discrete water samples at 85 stations in the Ross Sea from 13 February through 18 March 2013 (Fig. 1a). We used a rosette sampler fitted with 24 Niskin bottles and a Sea-Bird model SBE-911+ conductivity, temperature, and depth sensor. We also measured salinity on discrete underway and hydrocast samples at 25 °C using a Guildline 8400 Autosol four-electrode salinometer. The difference between the Autosol measurements and salinity from the conductivity sensor was less than 0.02. In this paper we use the hydrocast samples to evaluate the controls of seasonal surface Ω_{Ar} variability. The water column data will be further analyzed in upcoming papers.

We collected hydrocast samples for TA and DIC following the protocols of Dickson et al. (2007) and immediately added saturated mercuric chloride (<0.1 % by volume). For TA, we ran each sample within 12 h of collection using a second potentiometric titrator, a Metrohm 855 Robotic Titrosampler equipped with two 800 Metrohm Dosino syringe pumps (one 50 mL unit for rinsing and sample handling and one 5 mL unit for acid titration). The samples were prefiltered through 0.45 μm polyvinylidene fluoride filters and the estimated precision based on the CRMs ($n = 108$) is $\pm 1.5 \mu\text{mol kg}^{-1}$.

We measured DIC on hydrocast samples within ~ 4 h of collection without filtration. We acidified 1.25 mL of the sample using a custom-built injection system coupled to an infrared gas analyzer (LI-COR LI7000). As described by Long et al. (2011), the infrared absorption signal versus time is integrated for each stripped gas sample to yield a total mass of CO_2 . Samples were run in triplicate or greater and were calibrated using CRMs between every 3–4 unknowns. Micro-bubbles regularly appeared within injected samples due to sample warming between acquisition and DIC analysis. Each integration curve was visually inspected and integration curves that exhibited evidence for bubbles were rejected. The estimated precision based upon unknowns (> 3500 runs) and CRM replicates ($n = 855$) for cruise NPB-1302 is $\pm 3 \mu\text{mol kg}^{-1}$.

3.2 Carbon system calculations and crosschecks

We calculate Ω and DIC (hereafter called DIC_{calc}) for underway samples with CO2SYS for MATLAB (Lewis and Wallace, 1998; van Heuven et al., 2011) with TA, $p\text{CO}_2$, SST, and salinity as input variables. Calculations are only conducted for $p\text{CO}_2$ measured within 3 min of the TA measurement ($n = 1034$), the average cycle time for the automated $p\text{CO}_2$ measurements. We use the equilibrium constants of Mehrback et al. (1973) as refit by Dickson and Millero (1987) since previous studies have found that they are the optimal choice, including for Antarctic waters (Lee et al., 2000; Millero et al., 2002; McNeil et al., 2007). For the

hydrocast data, we calculate Ω using TA, DIC, temperature, and salinity as input variables.

As a means of internal quality control, we use the initial pH reading from the TA titration as a third carbon system parameter to crosscheck the accuracy of our Ω_{Ar} estimates. Ω_{Ar} calculated using TA and $p\text{CO}_2$ is 0.02 ± 0.07 greater than Ω_{Ar} calculated using TA and pH. In addition, DIC_{calc} using TA and $p\text{CO}_2$ is $2 \pm 7 \mu\text{mol kg}^{-1}$ lower than DIC_{calc} using TA and pH. Finally, measured $p\text{CO}_2$ is $4 \pm 14 \mu\text{atm}$ lower than $p\text{CO}_2$ calculated from TA and pH. These strong consistencies suggest that our $p\text{CO}_2$ and TA measurements are accurate. Our surface TA and DIC_{calc} measurements versus latitude for the Southern Ocean are within the ranges of other studies (Metzl et al., 2006; McNeil et al., 2007; Mattsdotter Björk et al., 2014).

We compare the TA measurements from the surface hydrocasts (<5 m deep) to the underway TA measurements made while the ship was still on station within ~ 15 min of when the surface samples were collected. The underway values are $3 \pm 5 \mu\text{mol kg}^{-1}$ higher than the hydrocast TA values.

3.3 Ross Sea and Southern Ocean calculations

The Ω_{Ar} of surface waters in the Ross Sea increases during the austral summer months (McNeil et al., 2010). We use DIC, TA, SST, and salinity to determine the controls on the seasonal cycle of surface water Ω_{Ar} . We normalize DIC and TA to a salinity of 34.5, the average salinity of the Ross Sea (hereafter called sDIC and sTA). Due to the deep convective mixing during the winter, we use the average sDIC and sTA concentrations of hydrocast samples collected from 200 to 400 m to determine winter water values (sDIC = $2221 \pm 5 \mu\text{mol kg}^{-1}$, sTA = $2338 \pm 3 \mu\text{mol kg}^{-1}$). While sDIC and sTA concentrations below 200 m are influenced by carbon export particularly in the summer and early autumn, observations show that sDIC and sTA concentrations are relatively uniform below 200 m across space and a given season (Table 1).

Following Hauri et al. (2013), the change in Ω_{Ar} of surface hydrocast samples (upper 10 m) from winter conditions can be expressed as

$$\Delta\Omega_{Ar} = \frac{\partial\Omega}{\partial\text{DIC}} \Delta\text{sDIC} + \frac{\partial\Omega}{\partial\text{TA}} \Delta\text{sTA} + \frac{\partial\Omega}{\partial T} \Delta T + \Delta S_{\Omega} + \text{Residuals}, \quad (2)$$

where

$$\Delta S_{\Omega} = \frac{\partial\Omega}{\partial S} \Delta S + \frac{\partial\Omega}{\partial\text{DIC}} \Delta\text{DIC}^s + \frac{\partial\Omega}{\partial\text{TA}} \Delta\text{TA}^s. \quad (3)$$

ΔsDIC and ΔsTA are the difference in sDIC and sTA for each sample from the winter value. The term ΔT is calculated using a winter SST of -1.89 °C (per Sweeney, 2003). ΔS_{Ω} represents the total contribution of salinity changes to $\Delta\Omega_{Ar}$.

Table 1. Mean values for sDIC concentrations below 200 m.

Data source	Early spring	Spring	Summer	Autumn
Sweeney et al. (2000)	2226 ± 3	2233 ± 3	2237 ± 3	2233 ± 5
Long et al. (2011)		2224 ± 5	2225 ± 4	
This paper				2220 ± 5

Since salinity between 200 and 400 m is variable across the Ross Sea (Orsi and Wiederwohl, 2009), ΔS is calculated as the difference between the salinity of a surface sample and the average salinity for samples from that station that are between 200 and 400 m.

ΔDIC^s and ΔTA^s represent changes to DIC and TA due to dilution/concentration from freshwater input and sea-ice processes:

$$\Delta \text{DIC}^s = \left[\text{DIC}_{200-400} \cdot \left(\frac{\text{Salinity}_{\text{surface sample}}}{\text{Salinity}_{200-400}} \right) - \text{DIC}_{200-400} \right] \quad (4)$$

$$\Delta \text{TA}^s = \left[\text{TA}_{200-400} \cdot \left(\frac{\text{Salinity}_{\text{surface sample}}}{\text{Salinity}_{200-400}} \right) - \text{TA}_{200-400} \right] \quad (5)$$

$\text{DIC}_{200-400}$, $\text{TA}_{200-400}$, and $\text{Salinity}_{200-400}$ are the average values for samples collected from 200 to 400 m calculated at each station.

The partial derivatives quantify the change in Ω_{Ar} per unit change in DIC, TA, temperature, and salinity. To determine the partial derivatives, we calculate Ω_{Ar} for all hydrocast samples within the upper 10 m using DIC, TA, temperature, and salinity as input parameters. We recalculate Ω_{Ar} after independently increasing DIC, TA, temperature, and salinity by one unit. The partial derivatives are the average difference between the initial Ω_{Ar} and the recalculated Ω_{Ar} .

We use the same equations to evaluate the relative importance of DIC, TA, temperature, and salinity on the variability of Ω_{Ar} from 75 to 55° S. For the Δ terms, we calculate the change in sDIC, sTA, temperature, and salinity from the mean of the first six underway measurements at 75° S. For Eqs. (4) and (5), instead of using DIC, TA, and salinity values from 200 to 400 m, we use the mean of the first six underway measurements at 75° S.

4 Results and discussion

4.1 Ω in the Ross Sea

Underway TA values range from 2268 to 2346 $\mu\text{mol kg}^{-1}$ (mean = 2314 ± 16 $\mu\text{mol kg}^{-1}$). Since TA strongly covaries with salinity ($R^2 = 0.86$, residual ± 6 $\mu\text{mol kg}^{-1}$), the lowest TA values are located in the west where the salinity is lowest (Fig. 1b). Values of sTA range from 2336 to 2386 $\mu\text{mol kg}^{-1}$ (mean = 2360 ± 7 $\mu\text{mol kg}^{-1}$) and are influenced by calcification/dissolution as well as phytoplankton photosynthesis since one unit of nitrate drawdown increases TA by one unit (Brewer and Goldman, 1978) (Fig. 1d).

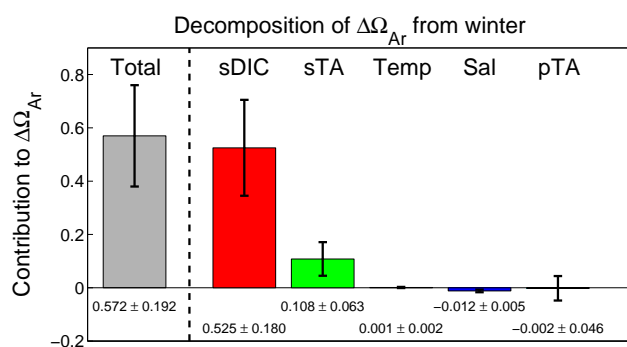


Figure 3. Contributions of sDIC, sTA, temperature, salinity, and PALK to changes in the aragonite saturation state (Ω_{Ar}) of surface waters from the winter to early autumn. Error bars represent ± 1 SD.

Surface $p\text{CO}_2$ values range from 162 to 354 μatm and are lower in the west due to late-season phytoplankton photosynthesis (Fig. 1e). Surface Ω_{Ar} ranges from 1.40 to 2.42 and Ω_{Ca} ranges from 2.24 to 3.89 (Fig. 2f). The highest Ω_{Ar} values are also located in the west. Phytoplankton photosynthesis increases Ω by both decreasing DIC and increasing TA.

Spatial and temporal variations in surface water Ω_{Ar} are mainly controlled by sDIC in the Ross Sea (Eq. (2), Fig. 3). The concentration of sDIC decreased by 58 ± 20 $\mu\text{mol kg}^{-1}$ from a winter value, causing Ω_{Ar} to increase by 0.5 ± 0.2. In addition, sTA increased by 11 ± 7 $\mu\text{mol kg}^{-1}$ during the preceding summer months, causing Ω_{Ar} to increase by 0.1 ± 0.1. Although there was a significant reduction in salinity compared to winter values (0.7 ± 0.3), Ω_{Ar} only decreased by ~0.01 due to this freshening since both DIC and TA concentrations were reduced. Lastly, the effect of temperature on Ω_{Ar} was negligible since the Ross Sea only experiences a 2 °C seasonal change in SSTs (Sweeney, 2003).

Two processes can reduce sDIC, calcification, and phytoplankton photosynthesis. To evaluate the importance of calcification, we use time-dependent changes in potential alkalinity (PALK = sNitrate + sTA) from a winter value (2367 ± 3 $\mu\text{mol kg}^{-1}$, defined as average value for all samples between 200 and 400 m). While TA will increase during photosynthesis due to nitrate drawdown, PALK will be conserved. Therefore, changes in PALK can be attributed to calcification and dissolution. The average ΔPALK from a winter concentration is negligible (0 ± 5 $\mu\text{mol kg}^{-1}$); therefore, calcification appears to be insignificant and the increase in sTA from winter conditions is largely driven by nitrate drawdown during photosynthesis. Earlier studies found that calcification contributed to only ~5% of the total seasonal DIC drawdown (Bates et al., 1998; Sweeney et al., 2000a). Therefore, we argue that photosynthesis exerts the dominant control on sDIC, sTA, and Ω_{Ar} . While the highest Ω_{Ar} value that we observed was 2.4, values up to ~4 have been observed during December–January (McNeil et al., 2010). By

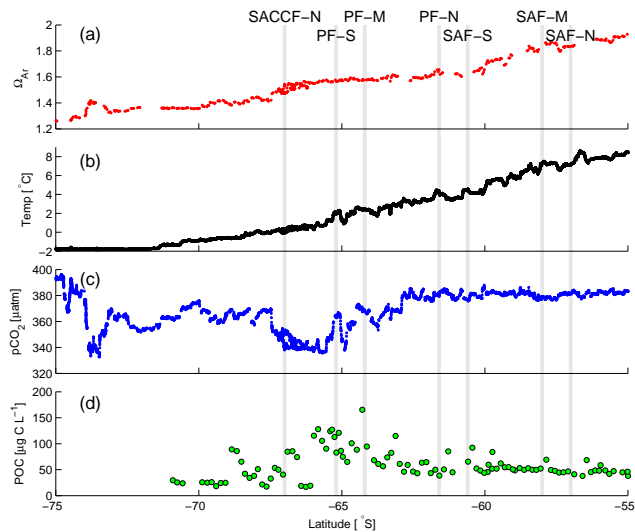


Figure 4. Surface water properties from a Southern Ocean transect, 20 March–2 April 2013: (a) aragonite saturation state (Ω_{Ar}), (b) SST, (c) pCO_2 , and (d) particulate organic carbon. The locations of the Subantarctic Front (SAF), the Polar Front (PF), and the southern Antarctic Circumpolar Current Front (SACCF) from Sokolov and Rintoul (2009) are indicated (gray lines).

the time we arrived in the Ross Sea, surface sDIC concentrations would have already increased relative to the summer due to enhanced air–sea CO_2 fluxes (Arrigo and van Dijken, 2007), deepening of the mixed layer (Sweeney, 2003), and remineralization of organic carbon (Sweeney et al., 2000b).

Mattsdotter Björk et al. (2014) also argue that phytoplankton photosynthesis is the major control on surface water Ω_{Ar} variability between the Ross Sea and the Antarctic Peninsula based upon the covariance of Ω_{Ar} and chlorophyll *a*. The largest contributor to seasonal Ω_{Ar} change in the Chukchi Sea in the Arctic is also phytoplankton photosynthesis (Bates et al., 2013). However, unlike the Ross Sea, numerous studies have also demonstrated aragonite undersaturation of surface waters in parts of the Arctic due to sea-ice melt and river runoff (Chierici and Fransson, 2009; Yamamoto-Kawai et al., 2009; Robbins et al., 2013).

4.2 Ω in the Southern Ocean

The spatial changes in Ω_{Ar} , SST, pCO_2 , and POC between 75 and 55° S are shown in Fig. 4. We also include the mean location of the fronts from Sokolov and Rintoul (2009) as they intersect our cruise track. The lowest Ω_{Ar} value is 1.25 ($\Omega_{Ca} = 2.00$) at 75° S, corresponding with the highest pCO_2 of $\sim 396 \mu\text{atm}$. Ω_{Ar} increases along the transect to reach a maximum of 1.93 ($\Omega_{Ca} = 3.04$) at 55° S. The changes in Ω_{Ar} are not always monotonic. In two regions changes in Ω_{Ar} can be attributed to enhanced primary production. Between 74 and 73° S, Ω_{Ar} first increases and then decreases by ~ 0.1 . This corresponds with a $40 \mu\text{atm}$ drop and then rise in pCO_2 .

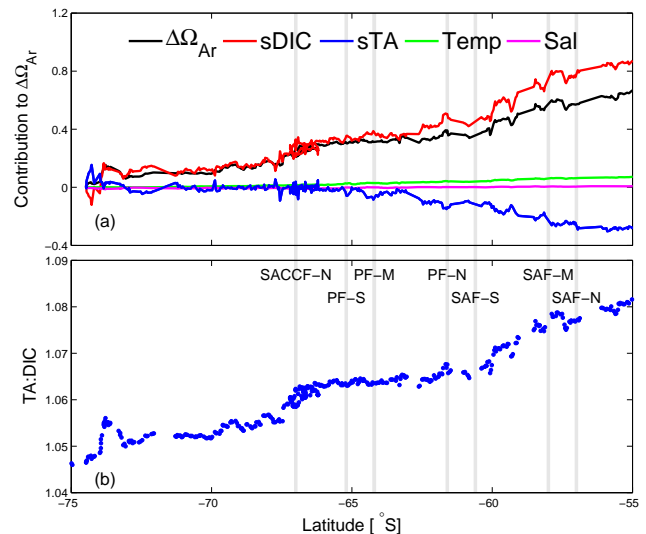


Figure 5. From surface water measurements along a Southern Ocean transect (a) contributions of changing sDIC (red), sTA (blue), temperature (green), and salinity (magenta) to changing aragonite saturation state (black, Ω_{Ar}) relative to the start of the transect and (b) TA to DIC ratios. The locations of the Subantarctic Front (SAF), the Polar Front (PF), and the southern Antarctic Circumpolar Current Front (SACCF) from Sokolov and Rintoul (2009) are indicated (gray lines).

Given that SST is constant, this localized increase in Ω_{Ar} is likely due to phytoplankton photosynthesis. This region may be along the Antarctic Slope Front that is known for higher biological activity (Jacobs, 1991). There is another step in Ω_{Ar} from ~ 1.4 to ~ 1.55 between 68 and 66° S across the SACCF-N. This step also corresponds with a decrease in pCO_2 from ~ 370 to $\sim 340 \mu\text{atm}$. Elevated POC concentrations between the SACCF-N and the PF-M correspond with these lower pCO_2 values and again indicate enhanced phytoplankton photosynthesis. Rubin (2003) also found that pCO_2 is reduced south of the PF (170° W) due to primary production.

To further gain insight into why Ω_{Ar} increases along our transect, we quantify the contribution of changing sDIC (calculated from TA and pCO_2), sTA, SST, and salinity to changing Ω_{Ar} (Fig. 5a). The dominant control is declining sDIC_{calc} from ~ 2240 to $\sim 2140 \mu\text{mol kg}^{-1}$ between 75 and 55° S, which causes Ω_{Ar} to increase by 0.87 if sTA, SST, and salinity are held constant (Fig. 6). Declining sTA from ~ 2340 to $\sim 2310 \mu\text{mol kg}^{-1}$ partially counters the influence of sDIC_{calc} and reduces Ω_{Ar} by 0.28. The influences of SST and salinity on Ω_{Ar} are minimal.

Ω_{Ar} variability is driven almost entirely by changes in sDIC_{calc} from 75° S to the PF-S. Between the PF-S and the SAF-N, variability in Ω_{Ar} is influenced by the opposing effects of sDIC_{calc} and sTA. The TA : DIC_{calc} ratio and Ω_{Ar} are constant between the PF-S and the SAF-S since both sDIC_{calc} and sTA decrease at the same rate (Fig. 5b).

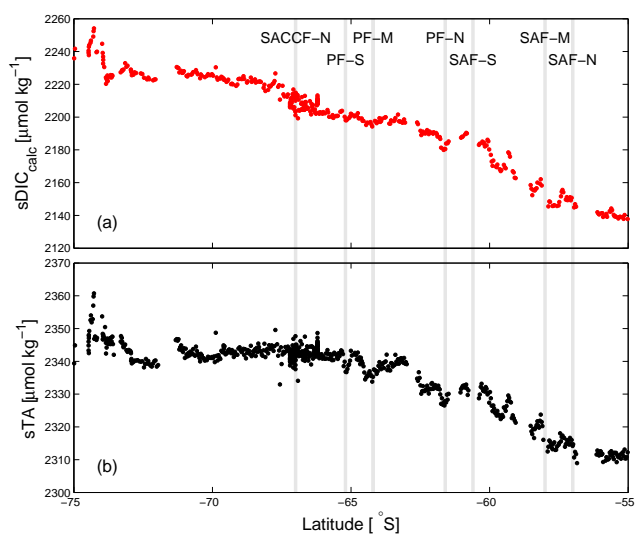


Figure 6. Measured surface water salinity normalized (a) DIC calculated from $p\text{CO}_2$, TA, temperature, and salinity and (b) TA. The locations of the Subantarctic Front (SAF), the Polar Front (PF), and the southern Antarctic Circumpolar Current Front (SACCF) from Sokolov and Rintoul (2009) are indicated (gray lines).

Between the SAF-S and the SAF-N, Ω_{Ar} increases since $s\text{DIC}_{\text{calc}}$ declines faster than $s\text{TA}$. North of the SAF-N, Ω_{Ar} variability is again driven by $s\text{DIC}_{\text{calc}}$. Ω_{Ar} increases due to a decrease in $s\text{DIC}_{\text{calc}}$ while $s\text{TA}$ remains constant.

We examine possible controls on $s\text{DIC}_{\text{calc}}$ along the transect. The concentration of $s\text{DIC}_{\text{calc}}$ is highest south of the PF-S due to upwelling of CDW (Fig. 6a). To evaluate the properties of CDW, we use data from the 2011 Repeat Hydrography Cruise SO4P, which is part of the US Climate Variability and Predictability (CLIVAR) program (Swift and Orsi, 2012) (available at: <http://www.clivar.org/resources/data/hydrographic>). We only use data from hydrocasts located between 168°E and 73°W where the bottom depth is $>1000\text{ m}$ (Fig. 2b). We reject the data from hydrocast 46(B) where the deep DIC data below 200 m are $\sim 30\ \mu\text{mol kg}^{-1}$ higher than the rest of the stations. Following Sweeney (2003), CDW is defined as centered on the level of maximum temperature below 150 m.

From this CLIVAR data set, CDW has a $s\text{DIC}$ value of $2243 \pm 3\ \mu\text{mol kg}^{-1}$. Between 75 and 74°S , $s\text{DIC}_{\text{calc}}$ concentration of surface water is also $2243 \pm 5\ \mu\text{mol kg}^{-1}$, indicating little modification to CDW and consistent with the observation that this region was covered by sea ice even during the summer of 2013. At 74°S $s\text{DIC}_{\text{calc}}$ drops to $\sim 2220\ \mu\text{mol kg}^{-1}$ and by 66°S , across the SACCF-N, $s\text{DIC}_{\text{calc}}$ drops to $\sim 2200\ \mu\text{mol kg}^{-1}$. This $40\ \mu\text{mol kg}^{-1}$ decrease in $s\text{DIC}_{\text{calc}}$ between Antarctica and the PF-S is consistent with the observed drops in $p\text{CO}_2$ that we attributed to photosynthesis. Rubin et al. (1998) also observed a $30\text{--}50\ \mu\text{mol kg}^{-1}$ decrease in $s\text{DIC}$ at 67°S in Pacific Antarctic

waters between winter and summer that they attribute to primary productivity.

$s\text{DIC}_{\text{calc}}$ continues to drop from $\sim 2220\ \mu\text{mol kg}^{-1}$ at the PF-S to $\sim 2140\ \mu\text{mol kg}^{-1}$ at 55°S , consistent with surface DIC measurements between 70 and 40°S compiled by McNeil et al. (2007). There are multiple factors likely responsible for this decrease in $s\text{DIC}_{\text{calc}}$. Both satellite (Arrigo et al., 2008) and in situ measurements (Reuer et al., 2007) show that annual primary productivity increases from south to north in the Southern Ocean. In addition, surface waters north of the PF advect northwards and accumulate a $s\text{DIC}$ deficit. Finally, warmer water holds less DIC while in equilibrium with the atmosphere. There is little net air–sea CO_2 flux between 75 and 55°S (except for net efflux at 60°S) since warming and increased biological production compensate each other (Takahashi et al., 2012).

We also examine possible controls on $s\text{TA}$ concentrations along the transect. The concentration of $s\text{TA}$ is also highest south of the PF-S due to upwelling of CDW. Based off the CLIVAR data set, the $s\text{TA}$ of CDW is $2334 \pm 3\ \mu\text{mol kg}^{-1}$. The $s\text{TA}$ of surface water between 74°S and the PF-S is $\sim 2340\ \mu\text{mol kg}^{-1}$, slightly higher than its CDW source (Fig. 6b). Nitrate drawdown during photosynthesis may explain the elevated $s\text{TA}$. Between 75 and 74°S , $s\text{TA}$ exceeds $2360\ \mu\text{mol kg}^{-1}$. One possible explanation is that ikaite ($\text{CaCO}_3 \cdot 6\text{H}_2\text{O}$), a mineral that has been observed directly and indirectly to precipitate in Antarctic sea ice (Dieckmann et al., 2008; Fransson et al., 2011), dissolved into surface waters during the summer causing $s\text{TA}$ concentrations to increase. Between the PF-S and SAF-N, $s\text{TA}$ drops to $2310\ \mu\text{mol kg}^{-1}$ where the concentrations level off. This drop appears to be in part due to the mixing of two end member water masses, AASW south of the PF-S and subantarctic surface water north of the SAF-N. The decreasing $s\text{TA}$ is consistent with the suggestion of Millero et al. (1998) that a negative linear relationship between $s\text{TA}$ and SST is due to colder water being indicative of greater upwelling of TA rich water.

This data set supports the argument that increased upwelling of CDW from strengthening westerly winds will increase OA in the Southern Ocean (Lenton et al., 2009). While the TA : DIC ratio for CDW is 1.040 ± 0.002 , the TA : DIC_{calc} ratio for surface waters between 75°S and the PF-S ranges from 1.046 to 1.064 (Fig. 5b). Therefore increased upwelling will lower the TA : DIC ratio and cause Ω_{Ar} to decrease.

4.3 Estimate of wintertime surface Ω_{Ar} values in the Ross Sea

Efforts to predict winter Ω_{Ar} undersaturation in the Ross Sea are complicated by the complete lack of carbon system measurements from the winter months in the Ross Sea.

McNeil et al. (2010) estimated winter surface water Ω_{Ar} by using the lowest observed Ω_{Ar} value from early spring when the Ross Sea is still covered by sea ice. They used mid-

October and early November carbon system measurements from the Joint Global Ocean Flux Study (JGOFS) (Sweeney et al., 2000b). Although sea-ice algae productivity peaks in November, its impact on water column DIC concentrations is likely to be negligible (Saenz and Arrigo, 2014). McNeil et al. (2010) found that early spring surface water Ω_{Ar} was ~ 1.2 . There was a single Ω_{Ar} value < 1.1 that they used as an initial condition along with the IPCC US92a scenario to predict that surface waters of the Ross Sea could begin to experience seasonally undersaturated conditions with respect to aragonite as early as 2015 if full equilibrium with rising atmospheric CO_2 is achieved. Based on a three-dimensional coupled ice, atmosphere, and ocean model (Arrigo et al., 2003, Tagliabue and Arrigo, 2005), McNeil et al. (2010) argued that only 35 % of the atmospheric CO_2 signal equilibrates with Ross Sea surface waters due to sea ice, upwelling of CDW, and short residence times, thereby delaying the onset of aragonite undersaturation until 2045. Decadal wintertime surface carbon system measurements do not exist to directly validate this disequilibrium assumption. In addition, McNeil et al. (2010) would inaccurately predict when the Ross Sea would become undersaturated with respect to aragonite if the minimum wintertime surface Ω_{Ar} value used was low due to measurement error.

To independently calculate Ω_{Ar} from early spring surface waters, we use the LDEO $p\text{CO}_2$ measurements from November 1994, 1997, 2005, and 2006 that are from the Ross Shelf (defined by the 1000 m isopleth) and are south of 74°S (Fig. 7a). The earliest $p\text{CO}_2$ measurements are from 16 November 1994, 17 November 1997, 6 November 2005, and 13 November 2006 when much of the Ross Sea is still covered in sea ice. The earliest measurements from 2005/06 are more likely to represent winter conditions since they are from 74°S as the NBP entered the Ross Sea. Conversely, the earliest measurements from 1994/97 are from the 76.5°S line, close to where the Ross Sea polynya opens up from.

We calculate wintertime TA in the Ross Sea by establishing a salinity–TA relationship using data from Bates et al. (1998), Sweeney et al. (2000b), and our own hydrocast TA measurements from the upper 10 m (Fig. A1 in the Appendix). Since one unit of nitrate drawdown increases TA by one unit, the TA measurements are adjusted to winter nitrate concentrations of $29\ \mu\text{mol kg}^{-1}$ (the mean nitrate concentration between 200 and 400 m from our cruise). The relationship between TA and salinity is consistent among these independent data sets and the standard deviation of the residuals for TA is $\pm 5\ \mu\text{mol kg}^{-1}$.

We calculate historical Ω_{Ar} using historical $p\text{CO}_2$ measurements, salinity-derived TA, SST, and salinity. Phosphate and silicate are set to the winter values of 2.1 and $79\ \mu\text{mol kg}^{-1}$, respectively. The TSG salinity data from the historical $p\text{CO}_2$ measurements appear reasonable and are uncalibrated. While the largest offset in TSG salinity compared with Autosal measurements is 0.3, such error is not typical. To test the possible impact of a poor salinity calibration, we

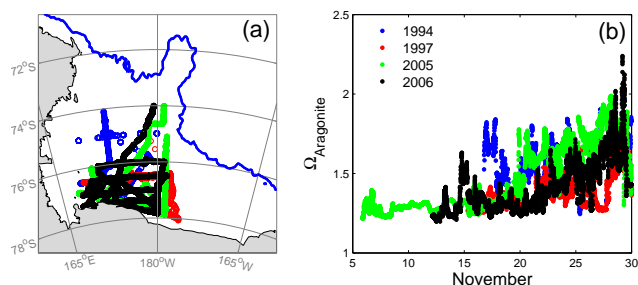


Figure 7. Estimating winter surface aragonite saturation states (Ω_{Ar}): (a) map of surface $p\text{CO}_2$ measurements from the LDEO $p\text{CO}_2$ database (<http://www.ldeo.columbia.edu/res/pi/CO2>) used in this study from November 1994 (blue), 1997 (red), 2005 (green), and 2006 (black). Blue line is the 1000 m isobath. (b) aragonite saturation state (Ω_{Ar}) of surface waters from November calculated from $p\text{CO}_2$, salinity-derived TA, temperature, and salinity.

recalculate Ω_{Ar} for all $p\text{CO}_2$ measurements after increasing salinity by 0.3. TA calculated from the observed TA–salinity relationship increases by $\sim 21\ \mu\text{mol kg}^{-1}$ and Ω_{Ar} increases by 0.024 ± 0.003 .

The lowest Ω_{Ar} measurements are 1.24 in 1994, 1.25 in 1997, 1.22 in 2005, and 1.20 in 2006 (Fig. 7b). Although Ω_{Ar} declines from 1994 to 2006, we have low confidence in any trend due to spatial–temporal sampling biases. The lowest Ω_{Ar} values are consistently between 1.2 and 1.3 as the ship crossed sea-ice-covered regions and open water that had experienced DIC drawdown. With the exception of a single measurement, the lowest 1996/97 Ω_{Ar} values from McNeil et al. (2010) are also ~ 1.2 . The similarity between the Ω_{Ar} values reported by McNeil et al. (2010) from 1996/97 and our 2005/06 values is consistent with their delayed acidification hypothesis.

A simple calculation also suggests that wintertime Ω_{Ar} values may be closer to 1.2 than 1.1. If salinity is 34.5, approximately the mean salinity of the water column, TA would be $2339\ \mu\text{mol kg}^{-1}$ based on the observed TA–salinity linear relationship. Sweeney (2003) estimates winter $p\text{CO}_2$ values of $\sim 425\ \mu\text{atm}$ based on deep $p\text{CO}_2$ measurements made during early spring. Setting salinity to 34.5, TA to $2339\ \mu\text{mol kg}^{-1}$, $p\text{CO}_2$ to $425\ \mu\text{atm}$, temperature to -1.89 , silicate to $79\ \mu\text{mol kg}^{-1}$, and phosphate to $2.1\ \mu\text{mol kg}^{-1}$ yields a Ω_{Ar} value of 1.22.

Although $p\text{CO}_2$ measurements of surface waters colder than -1.75°C south of 60°S typically reach $\sim 410\ \mu\text{atm}$ by September, Takahashi et al. (2009) present a few measurements of $\sim 450\ \mu\text{atm}$. Even if $p\text{CO}_2$ reaches $450\ \mu\text{atm}$ during winter in the Ross Sea, Ω_{Ar} would be 1.16 (with salinity at 34.5 and TA at $2339\ \mu\text{mol kg}^{-1}$). In order to obtain Ω_{Ar} of 1.1, $p\text{CO}_2$ would need to be $\sim 480\ \mu\text{atm}$, a value that appears unreasonably high given the available data sets from the Ross Sea.

Table 2. Water properties of CDW from McNeil et al. (2010) and CLIVAR.

Data source	Salinity	DIC ($\mu\text{mol kg}^{-1}$)	TA ($\mu\text{mol kg}^{-1}$)	PO ₄ ($\mu\text{mol kg}^{-1}$)	SiO ₄ ($\mu\text{mol kg}^{-1}$)	Ω_{Ar}
McNeil et al. (2010)	34.70 \pm 0.02	2255 \pm 1	2330	2.22 \pm 0.01	93.5 \pm 1.2	1.01
CLIVAR	34.71 \pm 0.02	2257 \pm 3	2348 \pm 4	2.21 \pm 0.04	95.6 \pm 6.0	1.18

McNeil et al. (2010) calculated the Ω_{Ar} of water arriving onto the Ross Shelf following the recipes of Jacobs et al. (1985): 50 % CDW, 25 % Tmin water (minimum temperature in upper 100 m), and 25 % AASW. To calculate the Ω_{Ar} of these three source water masses, they used hydrocast temperature, salinity, and DIC data collected during the austral winter of 1994 from north of the Ross Shelf as described in Sweeney (2003). They calculated that the average Ω_{Ar} of incoming water would be 1.08.

We independently calculate Ω_{Ar} of incoming water using the 2011 CLIVAR hydrocast data from north of the Ross Shelf between 168° E and 73° W as described earlier (Fig. 2b). The Ω_{Ar} of water in the upper 100 m (AASW and Tmin) from the CLIVAR data set is 1.36 ± 0.13 and the Ω_{Ar} of CDW (maximum temperature below 150 m) is 1.18 ± 0.03 (Fig. A2 in the Appendix). Even if 100 % of the incoming water onto the Ross Shelf is CDW, the Ω_{Ar} of this incoming water would be greater than 1.08. While most properties of CDW are similar between the 2011 CLIVAR data and the 1994 data used by McNeil et al. (2010), the TA of CDW from the CLIVAR data set is $18 \mu\text{mol kg}^{-1}$ higher (Table 2).

Another approach to estimate the Ω_{Ar} of winter surface waters is to use the properties of water below 200 m. For the TRACERS data, sTA below 200 m is $2338 \pm 2 \mu\text{mol kg}^{-1}$. For the JGOFS autumn cruise (NBP 97-3) sTA below 200 m is $2339 \pm 2 \mu\text{mol kg}^{-1}$. Using the CLIVAR data set, sTA of CDW from off the Ross Shelf is $2334 \pm 3 \mu\text{mol kg}^{-1}$. This consistency between independent data sets suggests that we can accurately estimate winter TA in the Ross Sea.

The range in sDIC below 200 m is much greater than that for sTA (Table 2). The lowest value is $2220 \pm 5 \mu\text{mol kg}^{-1}$ from our cruise and the highest is $2237 \pm 3 \mu\text{mol kg}^{-1}$ from the summer JGOFS cruise (NBP 97-01). This range in sDIC concentrations below 200 m is not surprising given that sDIC concentrations vary across the input water masses. In addition, sDIC concentrations below 200 m will be influenced by carbon export particularly in summer and early autumn and over multiple seasons' air-to-sea flux of CO₂.

Assuming that deep water concentrations of TA and DIC are relatively unmodified following wintertime deep convective mixing, we estimate the Ω_{Ar} of winter surface water by setting TA to $2338 \mu\text{mol kg}^{-1}$, salinity to 34.5, temperature to -1.89°C , phosphate to $2.1 \mu\text{mol kg}^{-1}$, and silicate to $79 \mu\text{mol kg}^{-1}$. If DIC concentrations are $2220 \mu\text{mol kg}^{-1}$, Ω_{Ar} would be 1.37. If sDIC concentrations are $2237 \mu\text{mol kg}^{-1}$, Ω_{Ar} would be 1.24 and $p\text{CO}_2$ would be 417 μatm .

These results are consistent with a study by Matson et al. (2014) where early spring Ω_{Ar} at 20 m depth calculated using pH and salinity-derived TA was 1.2–1.3 from Hut Point (bottom depth > 200 m) and Cape Evans (bottom depth < 30 m) in McMurdo Sound. In Prydz Bay, the lowest measured winter surface Ω_{Ar} values were also ~ 1.2 for both 1993–1995 (Gibson and Trull, 1999; McNeil et al., 2011) and 2010–2011 (Roden et al., 2013). Weeber et al. (2015) using hydrocast data estimated that the Ω_{Ar} of winter water in the Weddell Sea was ~ 1.3 . In the Mertz Polynya, the lowest Ω_{Ar} value at 100 m (below the mixed layer) was 1.2 (Shadwick et al., 2013). In Arthur Harbor on the western Antarctic Peninsula the lowest winter surface Ω_{Ar} value was 1.31 (Schram et al., 2015).

A few studies find Antarctic winter Ω_{Ar} values for surface water below 1.2. Hauri et al. (2015) used LDEO $p\text{CO}_2$ measurements and predicted TA from salinity to estimate winter Ω_{Ar} values of surface water in the western Antarctic Peninsula. They found that 20 % of Ω_{Ar} values were below 1.2 during the spring and winter, with a few winter values near undersaturation. It is not surprising that winter surface Ω_{Ar} values are lower in the Antarctic Peninsula than the Ross Sea given less sea ice in the Peninsula. In another study, Kapsenberg et al. (2015) report Ω_{Ar} at 18 m depth (bottom depth < 30 m) at two coastal sites in McMurdo Sound, the Jetty, and Cape Evans, for December–May and November–June, respectively, using pH and salinity-derived TA as input variables. The lowest Ω_{Ar} observations were from May at both sites and were 1.22 and 0.96 at the Jetty and Cape Evans. The maximum calculated $p\text{CO}_2$ was 559 at Cape Evans. The low Ω_{Ar} and high calculated $p\text{CO}_2$ values measured by Kapsenberg et al. (2015) may represent differences between coastal and open ocean systems – there may be a coastal amplification signal when sinking organic matter hits a shallow bed. Another possibility is that their carbon system time series, particularly at Cape Evans, is inaccurate. After conditioning and calibrating their pH measurements using discrete water samples, for logistical reasons Kapsenberg et al. (2015) could not collect additional validation samples during deployment or measure multiple carbon system parameters for crosscheck. Although the SeaFET pH sensors that they used are generally stable, they can drift (Bresnahan et al., 2014). Kapsenberg et al. (2015) have no means to assess possible pH sensor drift.

Following McNeil et al. (2010) and a Representative Concentration Pathway (RCP8.5) scenario (Meinshausen et al., 2011), we use the lowest Ω_{Ar} values from 2006 ($\Omega_{\text{Ar}} = 1.20$,

$p\text{CO}_2 = 428 \mu\text{atm}$, $\text{TA} = 2328 \mu\text{mol kg}^{-1}$, $\text{salinity} = 34.33$, $\text{SST} = -1.87^\circ\text{C}$, $\text{phosphate} = 2.1 \mu\text{mol kg}^{-1}$, $\text{silicate} = 79 \mu\text{mol kg}^{-1}$) to assess when the Ross Sea could become corrosive to aragonite. While shelf water salinity in the Ross Sea has declined by 0.03 decade^{-1} from 1958 to 2008 (Jacobs and Giulivi, 2010), we show that such rates of change will have inconsequential effects on Ω_{Ar} . For equilibrium conditions, surface waters in the Ross Sea would become corrosive to aragonite by 2040 (2092 for calcite) when atmospheric CO_2 concentrations exceed 485 ppm. In the disequilibrium scenario (McNeil et al., 2010), surface aragonite undersaturation state would occur by 2071 (2185 for calcite) when atmospheric CO_2 concentrations exceed 677 ppm.

Mattsdotter Björk et al. (2014) also predicted the onset of summertime aragonite in the Ross Sea. Their lowest Ω_{Ar} value was also ~ 1.2 and they estimated onset of undersaturation between 2026 and 2030 by increasing DIC by $10 \mu\text{mol kg}^{-1}$ per decade. This approach does not take into account air–sea CO_2 disequilibrium. In contrast, Hauck et al. (2010) found that only $3\text{--}5 \mu\text{mol kg}^{-1}$ of anthropogenic carbon accumulated per decade between 1992 and 2008 in shelf water of the Weddell Sea. In short, our analysis suggests that it may be possible to prevent future winter aragonite undersaturation of surface waters in the Ross Sea. For instance, CO_2 concentrations never exceed 543 ppm in the CO_2 stabilization scenario RCP4.5 (Meinshausen et al., 2011).

If the Ross Sea experiences aragonite undersaturation during winter in the future, live pteropod shells would start dissolving, making them more vulnerable to predation and bacterial infection (Bednaršek et al., 2012, 2014). In particular, pteropod larvae develop during the winter/spring (Gannefors et al., 2005; Hunt et al., 2008) and their shells have been shown to completely dissolve within weeks of exposure to aragonite undersaturation (Comeau et al., 2010). Declines in pteropod populations may reduce carbon export (Manno et al., 2010) and could have dramatic ecological effects up the food web.

Antarctic deep sea hydrocorals may also decline or disappear at the onset of aragonite undersaturation (Shadwick et al., 2014). In addition, the shells of post-mortem bivalves and brachiopods show significant dissolution within 2 months of exposure to undersaturated conditions, although live organisms may be able to compensate for this dissolution (McClin-tock et al., 2009). For instance, Cummings et al. (2011) show that the Antarctic bivalve *Laternula elliptica* can increase calcification in undersaturated conditions. However, the associated energy costs may be difficult to maintain over the long term, especially for larvae. Stumpp et al. (2012) shows that while echinoid larvae can maintain calcification in high $p\text{CO}_2$ treatments, increased energetic costs reduce growth

rates and ultimately increase mortality. Larvae of the Antarctic sea urchin *Sterechinus neumayeri* and sea star *Odontaster validus* are smaller and exhibit abnormal development under elevated $p\text{CO}_2$ treatments (Byrne et al., 2013; Gonzalez-Bernat et al., 2013; Yu et al., 2013). In addition, the synergistic effects of warming and OA could impact echinoderm fertilization and embryo development (Ericson et al., 2012). Although it is not clear to what extent species may acclimatize or adapt (e.g., Suckling et al., 2015), the onset of aragonite undersaturation during winter months may have profound impacts on the Ross Sea ecosystem.

5 Conclusions

Our study demonstrates the possibility of setting up underway TA measurement systems. Although our system was relatively unattended, carbon system crosschecks and comparisons between hydrocast and underway data indicate that our measurements were accurate. Similar underway TA systems could be set up on scientific vessels and ships of opportunity in undersampled regions of the world's oceans.

We find that the seasonal increase in Ω_{Ar} in the Ross Sea by early autumn is driven almost entirely by phytoplankton photosynthesis. In the Southern Ocean between the Ross Sea and Chile we find that Ω_{Ar} also increases mainly due to declining DIC_{calc} although declining TA partially counters the influence of declining DIC_{calc} . The influences of SST and salinity on Ω_{Ar} are minimal in the Ross Sea and on our Southern Ocean transect.

We establish a salinity–TA relationship for the winter that is consistent across independent data sets. Using historical $p\text{CO}_2$ measurements from early spring along with TA predicted from salinity, we argue that it is unlikely that the Ross Sea actually experienced winter surface Ω_{Ar} values of ~ 1.1 during 1996 (as per McNeil et al., 2010) and that a Ω_{Ar} value of ~ 1.2 may more accurately represent current winter conditions.

Since predictions are sensitive to current surface wintertime Ω_{Ar} values as well as the extent of disequilibrium, highly accurate carbon system measurements from the winter are crucial. It is also essential to measure more than two carbon system parameters for crosscheck. For instance, pH and $p\text{CO}_2$ sensors on moorings and floats could be used with TA predicted from salinity to calculate Ω during the winter.

Our analysis indicates that the Ross Sea will not experience aragonite undersaturation until the year 2070 following RCP8.5. In some CO_2 stabilization scenarios, including RCP4.5 (Meinshausen et al., 2011), the Ross Sea may avoid becoming corrosive to aragonite.

Appendix A

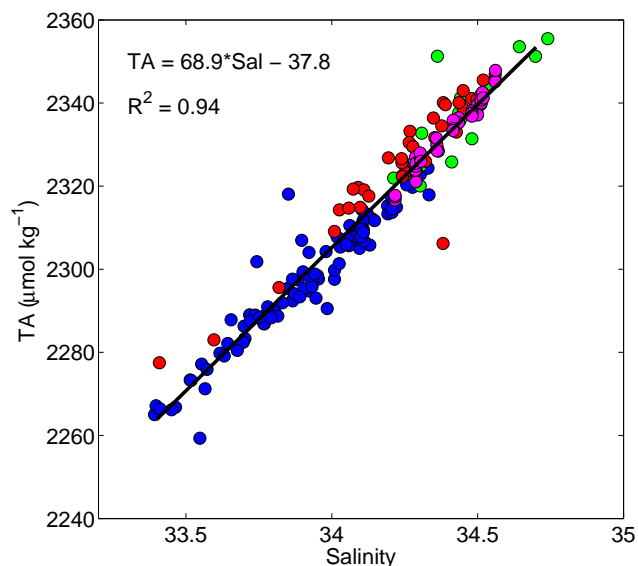


Figure A1. Linear regression between TA and salinity with surface data from February to March 2013 (blue; this study), November to December 1994 (green; Bates et al., 1998), December to January 1995/1996 (red; Bates et al., 1998), and April 1997 (magenta; Sweeney et al., 2000a). TA has been corrected to a nitrate concentration of $29 \mu\text{mol kg}^{-1}$ to account for the effects of nitrate drawdown on TA (Brewer and Goldman, 1976).

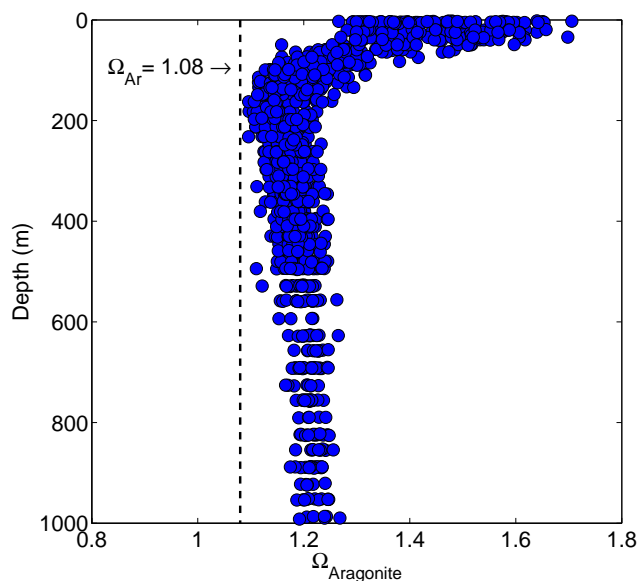


Figure A2. Profiles of aragonite saturation state (Ω_{Ar}) from off the Ross Shelf (see Fig. 2b) from the CLIVAR program (NBP 11-02) calculated from TA, DIC, temperature, and salinity at surface pressures.

The Supplement related to this article is available online at doi:10.5194/bg-12-6881-2015-supplement.

Acknowledgements. This work was supported by the US NSF (OPP-1142044 to R. B. Dunbar) and a NSF graduate research fellowship grant (DGE-114747 to H. B. DeJong). We thank the captain and crew of the R/V *Nathaniel B. Palmer*. We are grateful to S. Bercovici for the nitrate data. The comments of two anonymous reviewers greatly improved this paper.

Edited by: L. Bopp

References

- Accornero, A., Manno, C., Esposito, F., and Gambi, M. C.: The vertical flux of particulate matter in the polynya of Terra Nova Bay. Part II. Biological components, *Antarct. Sci.*, 15, 175–188, doi:10.1017/S0954102003001214, 2003.
- Andersson, A. J., Mackenzie, F. T., and Gattuso, J.-P.: Effects of ocean acidification on benthic processes, organisms, and ecosystems, in: *Ocean Acidification*, edited by: Gattuso, J.-P. and Hanson, L., Oxford University Press, New York, USA, 122–153, 2011.
- Archer, D., Eby, M., Brovkin, V., Ridgwell, A., Cao, L., Mikolajewicz, U., Caldeira, K., Matsumoto, K., Munhoven, G., Montenegro, A., and Tokos, K.: Atmospheric Lifetime of Fossil Fuel Carbon Dioxide, *Annu. Rev. Earth Pl. Sc.*, 37, 117–134, doi:10.1146/annurev.earth.031208.100206, 2009.
- Arrigo, K. R. and McClain, C. R.: Spring Phytoplankton Production in the Western Ross Sea, *Science*, 266, 261–263, doi:10.1126/science.266.5183.261, 1994.
- Arrigo, K. R. and van Dijken, G. L.: Phytoplankton dynamics within 37 Antarctic coastal polynya systems, *J. Geophys. Res.*, 108, 3271, doi:10.1029/2002JC001739, 2003.
- Arrigo, K. R. and van Dijken, G. L.: Annual changes in sea-ice, chlorophyll a, and primary production in the Ross Sea, Antarctica, *Deep-Sea Res. Pt. II*, 51, 117–138, doi:10.1016/j.dsr2.2003.04.003, 2004.
- Arrigo, K. R. and van Dijken, G. L.: Interannual variation in air-sea CO₂ flux in the Ross Sea, Antarctica: A model analysis, *J. Geophys. Res.*, 112, 1–16, doi:10.1029/2006JC003492, 2007.
- Arrigo, K. R., Robinson, D. H., Worthen, D. L., Dunbar, R. B., DiTullio, G. R., VanWoert, M., and Lizotte, M. P.: Phytoplankton community structure and the drawdown of nutrients and CO₂ in the Southern Ocean, *Science*, 283, 365–367, doi:10.1126/science.283.5400.365, 1999.
- Arrigo, K. R., Worthen, D. L., and Robinson, D. H.: A coupled ocean-ecosystem model of the Ross Sea: 2. Iron regulation of phytoplankton taxonomic variability and primary production, *J. Geophys. Res.*, 108, 3231, doi:10.1029/2001JC000856, 2003.
- Arrigo, K. R., van Dijken, G. L., and Bushinsky, S.: Primary production in the Southern Ocean, 1997–2006, *J. Geophys. Res.*, 113, C08004, doi:10.1029/2007JC004551, 2008.
- Bates, N. R., Hansell, D. A., Carlson, C. A., and Gordon, L. I.: Distribution of CO₂ species, estimates of net community production, and air-sea CO₂ exchange in the Ross Sea polynya, *J. Geophys. Res.*, 103, 2883–2896, doi:10.1029/97jc02473, 1998.
- Bates, N. R., Orchowka, M. I., Garley, R., and Mathis, J. T.: Summertime calcium carbonate undersaturation in shelf waters of the western Arctic Ocean – how biological processes exacerbate the impact of ocean acidification, *Biogeosciences*, 10, 5281–5309, doi:10.5194/bg-10-5281-2013, 2013.
- Bednaršek, N., Tarling, G. A., Bakker, D. C. E., Fielding, S., Jones, E. M., Venables, H. J., Ward, P., Kuzirian, A., Lézé, B., Feely, R. A., and Murphy, E. J.: Extensive dissolution of live pteropods in the Southern Ocean, *Nat. Geosci.*, 5, 881–885, doi:10.1038/ngeo1635, 2012.
- Bednaršek, N., Tarling, G. A., Bakker, D. C., Fielding, S., and Feely, R. A.: Dissolution dominating calcification process in polar pteropods close to the point of aragonite undersaturation, *PLoS One*, 9, e109183, doi:10.1371/journal.pone.0109183, 2014.
- Bresnahan, P. J., Martz, T. R., Takeshita, Y., Johnson, K. S., and Lashomb, M.: Best practices for autonomous measurement of seawater pH with the Honeywell Durafet, *Methods Oceanogr.*, 9, 1–33, doi:10.1016/j.mio.2014.08.003, 2014.
- Brewer, P. G. and Goldman, J. C.: Alkalinity changes generated by phytoplankton growth, *Limnol. Oceanogr.*, 21, 108–117, doi:10.4319/lo.1976.21.1.0108, 1976.
- Byrne, M., Ho, M. A., Koleits, L., Price, C., King, C. K., Virtue, P., Tilbrook, B., and Lamare, M.: Vulnerability of the calcifying larval stage of the Antarctic sea urchin *Stereochinus neumayeri* to near-future ocean acidification and warming, *Glob. Change Biol.*, 19, 2264–2275, doi:10.1111/gcb.12190, 2013.
- Caldeira, K. and Wickett, M. E.: Oceanography: anthropogenic carbon and ocean pH, *Nature*, 425, p. 365, doi:10.1038/425365a, 2003.
- Chierici, M. and Fransson, A.: Calcium carbonate saturation in the surface water of the Arctic Ocean: undersaturation in freshwater influenced shelves, *Biogeosciences*, 6, 2421–2431, doi:10.5194/bg-6-2421-2009, 2009.
- Collier, R., Dymond, J., Honjo, S., Manganini, S., Francois, R., and Dunbar, R.: The vertical flux of biogenic and lithogenic material in the Ross Sea: Moored sediment trap observations 1996–1998, *Deep-Sea Res. Pt. II*, 47, 3491–3520, doi:10.1016/S0967-0645(00)00076-X, 2000.
- Comeau, S., Gorsky, G., Alliouane, S., and Gattuso, J.-P.: Larvae of the pteropod *Cavolinia inflexa* exposed to aragonite undersaturation are viable but shell-less, *Mar. Biol.*, 157, 2341–2345, doi:10.1007/s00227-010-1493-6, 2010.
- Cummings, V., Hewitt, J., Van Rooyen, A., Currie, K., Beard, S., Thrush, S., Norkko, J., Barr, N., Heath, P., Halliday, N. J., Sedcole, R., Gomez, A., McGraw, C., and Metcalf, V.: Ocean acidification at high latitudes: potential effects on functioning of the Antarctic bivalve *Laternula elliptica*, *PLoS ONE*, 6, e16069, doi:10.1371/journal.pone.0016069, 2011.
- Dickson, A. G.: The carbon dioxide system in seawater: equilibrium chemistry and measurements, in: *Guide to Best Practices in Ocean Acidification Research and Data Reporting*, edited by: Riebesell, U., Fabry, V. J., Hansson, L., and Gattuso, J.-P., Office for Official Publications of the European Communities, Luxembourg, 17–40, 2010.
- Dickson, A. G. and Millero, F. J.: A comparison of the equilibrium constants for the dissociation of carbonic acid in seawater media, *Deep-Sea Res.*, 34, 1733–1743, doi:10.1016/0198-0149(87)90021-5, 1987.

- Dickson, A. G., Afghan, J. D., and Anderson, G. C.: Reference materials for oceanic CO₂ analysis: a method for the certification of total alkalinity, *Mar. Chem.*, 80, 185–197, doi:10.1016/S0304-4203(02)00133-0, 2003.
- Dickson, A. G., Sabine, C. L., and Christian, J. R.: Guide to best practices for ocean CO₂ measurements, *PICES Spec. Publ.*, 3, p. 191, doi:10.1159/000331784, 2007.
- Dieckmann, G. S., Nehrke, G., Papadimitriou, S., Göttlicher, J., Steininger, R., Kennedy, H., Wolf-Gladrow, D., and Thomas, D. N.: Calcium carbonate as ikaite crystals in Antarctic sea ice, *Geophys. Res. Lett.*, 35, 35–37, doi:10.1029/2008GL033540, 2008.
- Dinniman, M. S., Klinck, J. M., and Smith, W. O.: A model study of Circumpolar Deep Water on the West Antarctic Peninsula and Ross Sea continental shelves, *Deep-Sea Res. Pt. II*, 58, 1508–1523, doi:10.1016/j.dsr2.2010.11.013, 2011.
- Ericson, J. A., Ho, M. A., Miskelly, A., King, C. K., Virtue, P., Tilbrook, B., and Byrne, M.: Combined effects of two ocean change stressors, warming and acidification, on fertilization and early development of the Antarctic echinoid *Sterechninus neumayeri*, *Polar Biol.*, 35, 1027–1034, doi:10.1007/s00300-011-1150-7, 2012.
- Feely, R., Doney, S., and Cooley, S.: Ocean Acidification: Present Conditions and Future Changes in a High-CO₂ World, *Oceanography*, 22, 36–47, doi:10.5670/oceanog.2009.95, 2009.
- Feng, Y., Hare, C. E., Rose, J. M., Handy, S. M., DiTullio, G. R., Lee, P. A., Smith, W. O., Peloquin, J., Tozzi, S., Sun, J., Zhang, Y., Dunbar, R. B., Long, M. C., Sohst, B., Lohan, M., and Hutchins, D. A.: Interactive effects of iron, irradiance and CO₂ on Ross Sea phytoplankton, *Deep-Sea Res. Pt. I*, 57, 368–383, doi:10.1016/j.dsr.2009.10.013, 2010.
- Foster, B. A. and Montgomery, J. C.: Planktivory in benthic nototheniid fish in McMurdo Sound, Antarctica, *Environ. Biol. Fish.*, 36, 313–318, doi:10.1007/BF00001727, 1993.
- Fransson, A., Chierici, M., Yager, P. L., and Smith, W. O.: Antarctic sea ice carbon dioxide system and controls, *J. Geophys. Res.*, 116, C12035, doi:10.1029/2010JC006844, 2011.
- Gannefors, C., Boer, M., Kattner, G., Graeve, M., Eiane, K., Gulliksen, B., Hop, H., and Falk-Petersen, S.: The Arctic sea butterfly *Limacina helicina*: lipids and life strategy, *Mar. Biol.*, 147, 169–177, doi:10.1007/s00227-004-1544-y, 2005.
- Gibson, J. A. E. and Trull, T. W.: Annual cycle of fCO₂ under sea-ice and in open water in Prydz Bay, East Antarctica, *Mar. Chem.*, 66, 187–200, doi:10.1016/S0304-4203(99)00040-7, 1999.
- Gonzalez-Bernat, M. J., Lamare, M., and Barker, M.: Effects of reduced seawater pH on fertilisation, embryogenesis and larval development in the Antarctic seastar *Odontaster validus*, *Polar Biol.*, 36, 235–247, doi:10.1007/s00300-012-1255-7, 2013.
- Gordon, L. I., Codispoti, L. A., Jennings, J. C., J., Millero, F. J., Morrison, J. M., and Sweeney, C.: Seasonal evolution of hydrographic properties in the Ross Sea, Antarctica, 1996–1997, *Deep-Sea Res. Pt. II*, 47, 3095–3117, doi:10.1016/S0967-0645(00)00060-6, 2000.
- Hauk, J., Hoppema, M., Bellerby, R. G. J., Völker, C., and Wolf-Gladrow, D.: Data-based estimation of anthropogenic carbon and acidification in the Weddell Sea on a decadal timescale, *J. Geophys. Res.-Oceans*, 115, 1–14, doi:10.1029/2009JC005479, 2010.
- Hauk, J., Arrigo, K. R., Hoppema, M., Van Dijken, G. L., Völker, C. and Wolf-Gladrow, D. A.: Insignificant buffering capacity of Antarctic shelf carbonates, *Global Biogeochem. Cy.*, 27, 11–20, doi:10.1029/2011GB004211, 2013.
- Hauri, C., Gruber, N., Vogt, M., Doney, S. C., Feely, R. A., Lachkar, Z., Leinweber, A., McDonnell, A. M. P., Munnich, M., and Plattner, G.-K.: Spatiotemporal variability and long-term trends of ocean acidification in the California Current System, *Biogeosciences*, 10, 193–216, doi:10.5194/bg-10-193-2013, 2013.
- Hauri, C., Doney, S. C., Takahashi, T., Erickson, M., Jiang, G., and Ducklow, H. W.: Two decades of inorganic carbon dynamics along the Western Antarctic Peninsula, *Biogeosciences Discuss.*, 12, 6929–6969, doi:10.5194/bgd-12-6929-2015, 2015.
- Hopkins, T. L.: Midwater food web in McMurdo Sound, Ross Sea, Antarctica, *Mar. Biol.*, 96, 93–106, doi:10.1007/BF00394842, 1987.
- Hunt, B. P. V., Pakhomov, E. A., Hosie, G. W., Siegel, V., Ward, P., and Bernard, K.: Pteropods in Southern Ocean ecosystems, *Prog. Oceanogr.*, 78, 193–221, doi:10.1016/j.pocean.2008.06.001, 2008.
- IPCC AR5 WG1, Climate Change 2013: The Physical Science Basis. Contribution of Working Group I to the Fifth Assessment Report of the Intergovernmental Panel on Climate Change Rep., Cambridge, UK and New York, NY, USA, 1535 pp., 2013.
- Jacobs, S. S.: On the nature and significance of the Antarctic Slope Front, *Mar. Chem.*, 35, 9–24, doi:10.1016/S0304-4203(09)90005-6, 1991.
- Jacobs, S. S. and Giulivi, C. F.: Large multidecadal salinity trends near the Pacific-Antarctic continental margin, *J. Climate*, 23, 4508–4524, doi:10.1175/2010JCLI3284.1, 2010.
- Jacobs, S. S., Fairbanks, R. G., and Horibe, Y.: Origin and evolution of water masses near the Antarctic continental margin: evidence from H₂¹⁸O/H₂¹⁶O ratios in seawater, in: *Oceanography of the Antarctic Continental Shelf*, Antarctic Research Series, 43, edited by: Jacobs, S. S., American Geophysical Union, Washington, DC, USA, 59–85, 1985.
- Kapsenberg, L., Kelley, A. L., Shaw, E. C., Martz, T. R., and Hofmann, G. E.: Near-shore Antarctic pH variability has implications for the design of ocean acidification experiments, *Sci. Rep.*, 5, 9638, doi:10.1038/srep09638, 2015.
- Kawaguchi, S., Ishida, A., King, R., Raymond, B., Waller, N., Constable, A., Nicol, S., Wakita, M., and Ishimatsu, A.: Risk maps for Antarctic krill under projected Southern Ocean acidification, *Nat. Clim. Chang.*, 3, 843–847, doi:10.1038/nclimate1937, 2013.
- Knap, A., Michaels, A., Close, A., Ducklow, H., and A. Dickson: Protocols for the Joint Global Ocean Flux Study (JGOFS) Core Measurements, *JGOFS Rep.*, 19, 1–170, 1996.
- Kohut, J., Hunter, E., and Huber, B.: Small-scale variability of the cross-shelf flow over the outer shelf of the Ross Sea, *J. Geophys. Res.-Oceans*, 118, 1863–1876, doi:10.1002/jgrc.20090, 2013.
- La Mesa, M., Vacchi, M., and Zunini Sertorio, T.: Feeding plasticity of *Trematomus newnesi* (Pisces, Nototheniidae) in Terra Nova Bay, Ross Sea, in relation to environmental conditions, *Polar Biol.*, 23, 38–45, doi:10.1007/s003000050006, 2000.
- La Mesa, M., Eastman, J. T., and Vacchi, M.: The role of nototheniid fish in the food web of the Ross Sea shelf waters: A review, *Polar Biol.*, 27, 321–338, doi:10.1007/s00300-004-0599-z, 2004.
- Lee, K., Millero, F. J., Byrne, R. H., Feely, R. A., and Wanninkhof, R.: The recommended dissociation constants for carbonic acid in seawater, *Geophys. Res. Lett.*, 27, 229–232, doi:10.1029/1999GL002345, 2000.

- Lenton, A., Codron, F., Bopp, L., Metzl, N., Cadule, P., Tagliabue, A., and Le Sommer, J.: Stratospheric ozone depletion reduces ocean carbon uptake and enhances ocean acidification, *Geophys. Res. Lett.*, 36, L12606, doi:10.1029/2009GL038227, 2009.
- Lewis, E. and Wallace, D. W. R.: Program Developed for CO₂ System Calculations ORNL/CDIAC-105, Carbon Dioxide Information Analysis Centre, Oakridge National Laboratory, US Department of Energy, Oakridge, TN, USA, 1998.
- Long, M. C., Dunbar, R. B., Tortell, P. D., Smith, W. O., Mucciarone, D. A., and Ditullio, G. R.: Vertical structure, seasonal drawdown, and net community production in the Ross Sea, Antarctica, *J. Geophys. Res.-Oceans*, 116, 1–19, doi:10.1029/2009JC005954, 2011.
- Manno, C., Tirelli, V., Accornero, A., and Fonda Umani, S.: Importance of the contribution of limacina helicina faecal pellets to the carbon pump in terra nova bay (Antarctica), *J. Plankton Res.*, 32, 145–152, doi:10.1093/plankt/fbp108, 2010.
- Matson, P. G., Washburn, L., Martz, T. R., and Hofmann, G. E.: Abiotic versus Biotic Drivers of Ocean pH Variation under Fast Sea Ice in McMurdo Sound, Antarctica, 9, e107239, doi:10.1371/journal.pone.0107239, 2014.
- Mattsdotter Björk, M., Fransson, A., Torstensson, A., and Chierici, M.: Ocean acidification state in western Antarctic surface waters: controls and interannual variability, *Biogeosciences*, 11, 57–73, doi:10.5194/bg-11-57-2014, 2014.
- McClintock, J. B., Angus, R. A., McDonald, M. R., Amsler, C. D., Catledge, S. A., and Vohra, Y. K.: Rapid dissolution of shells of weakly calcified antarctic benthic macroorganisms indicates high vulnerability to ocean acidification, *Antarct. Sci.*, 21, 449–456, doi:10.1017/S0954102009990198, 2009.
- McClintock, J. B., Amsler, M. O., Angus, R. A., Challener, R. C., Schram, J. B., Amsler, C. D., Mah, C. L., Cuce, J., and Baker, B. J.: The Mg-Calcite Composition of Antarctic Echinoderms: Important Implications for Predicting the Impacts of Ocean Acidification, *J. Geol.*, 119, 457–466, doi:10.1086/660890, 2011.
- McNeil, B. I. and Matear, R. J.: Southern Ocean acidification: a tipping point at 450-ppm atmospheric CO₂, *P. Natl. Acad. Sci. USA*, 105, 18860–18864, doi:10.1073/pnas.0806318105, 2008.
- McNeil, B. I., Metzl, N., Key, R. M., Matear, R. J., and Corbiere, A.: An empirical estimate of the Southern Ocean air-sea CO₂ flux, *Global Biogeochem. Cy.*, 21, GB3011, doi:10.1029/2007GB002991, 2007.
- McNeil, B. I., Tagliabue, A., and Sweeney, C.: A multi-decadal delay in the onset of corrosive acidified waters in the Ross Sea of Antarctica due to strong air-sea CO₂ disequilibrium, *Geophys. Res. Lett.*, 37, 1–5, doi:10.1029/2010GL044597, 2010.
- McNeil, B. I., Sweeney, C., and Gibson, J. A. E.: Short Note: Natural seasonal variability of aragonite saturation state within two Antarctic coastal ocean sites, *Antarct. Sci.*, 23, 411–412, doi:10.1017/S0954102011000204, 2011.
- Mehrback, C., Culbertson, C. H., Hawley, J. E., and Pytkowicz, R. M.: Measurement of the apparent dissociation constants of carbonic acid in seawater at atmospheric pressure, *Limnol. Oceanogr.*, 18, 897–907, doi:10.4319/lo.1973.18.6.0897, 1973.
- Meinshausen, M., Smith, S. J., Calvin, K., Daniel, J. S., Kainuma, M. L. T., Lamarque, J., Matsumoto, K., Montzka, S. A., Raper, S. C. B., Riahi, K., Thomson, A., Velders, G. J. M. and van Vuuren, D. P. P.: The RCP greenhouse gas concentrations and their extensions from 1765 to 2300, *Clim. Change*, 109, 213–241, doi:10.1007/s10584-011-0156-z, 2011.
- Metzl, N., Brunet, C., Jabaud-Jan, A., Poisson, A., and Schauer, B.: Summer and winter air-sea CO₂ fluxes in the Southern Ocean, *Deep-Sea Res. Pt. I*, 53, 1548–1563, doi:10.1016/j.dsr.2006.07.006, 2006.
- Millero, F. J., Lee, K., and Roche, M.: Distribution of alkalinity in the surface waters of the major oceans, *Mar. Chem.*, 60, 111–130, 1998.
- Millero, F. J., Pierrot, D., Lee, K., Wanninkhof, R., Feely, R., Sabine, C. L., Key, R. M. and Takahashi, T.: Dissociation constants for carbonic acid determined from field measurements, *Deep-Sea Res. Pt. I*, 49, 1705–1723, doi:10.1016/S0967-0637(02)00093-6, 2002.
- Moy, A. D., Howard, W. R., Bray, S. G., and Trull, T. W.: Reduced calcification in modern Southern Ocean planktonic foraminifera, *Nat. Geosci.*, 2, 276–280, doi:10.1038/ngeo460, 2009.
- Mucci, A.: The solubility of calcite and aragonite in seawater at various salinities, temperatures, and one atmosphere total pressure, *Am. J. Sci.*, 283, 780–799, doi:10.2475/ajs.283.7.780, 1983.
- Orr, J. C., Fabry, V. J., Aumont, O., Bopp, L., Doney, S. C., Feely, R. A., Gnanadesikan, A., Gruber, N., Ishida, A., Joos, F., Key, R. M., Lindsay, K., Maier-Reimer, E., Matear, R., Monfray, P., Mouchet, A., Najjar, R. G., Plattner, G.-K., Rodgers, K. B., Sabine, C. L., Sarmiento, J. L., Schlitzer, R., Slater, R. D., Totterdell, I. J., and Weirig, M.-F., Yamanaka, Y. and Yool, A.: Anthropogenic ocean acidification over the twenty-first century and its impact on calcifying organisms, *Nature*, 437, 681–686, doi:10.1038/nature04095, 2005.
- Orsi, A. H. and Wiederwohl, C. L.: A recount of Ross Sea waters, *Deep-Sea Res. Pt. II*, 56, 778–795, doi:10.1016/j.dsr.2.2008.10.033, 2009.
- Orsi, A. H., Whitworth, T., and Nowlin, W. D.: On the meridional extent and fronts of the Antarctic Circumpolar Current, *Deep-Sea Res. Pt. I*, 42, 641–673, doi:10.1016/0967-0637(95)00021-W, 1995.
- Petty, A. A., Holland, P. R., and Feltham, D. L.: Sea ice and the ocean mixed layer over the Antarctic shelf seas, *The Cryosphere*, 8, 761–783, doi:10.5194/tc-8-761-2014, 2014.
- Reuer, M. K., Barnett, B. A., Bender, M. L., Falkowski, P. G., and Hendricks, M. B.: New estimates of Southern Ocean biological production rates from O₂/Ar ratios and the triple isotope composition of O₂, *Deep-Sea Res. Pt. I*, 54, 951–974, doi:10.1016/j.dsr.2007.02.007, 2007.
- Riebesell, U., Zondervan, I., Rost, B., Tortell, P. D., Zeebe, R. E., and Morel, F. M.: Reduced calcification of marine plankton in response to increased atmospheric CO₂, *Nature*, 407, 364–367, doi:10.1038/35030078, 2000.
- Rintoul, S., Hughes, C., and Olbers, D.: The Antarctic Circumpolar Current System, in: *Ocean Circulation and Climate*, edited by: Siedler, G., Church, J., and Gould, J., Elsevier, New York, USA, 271–301, 2001.
- Rivaró, P., Messa, R., Ianni, C., Magi, E., and Budillon, G.: Distribution of total alkalinity and pH in the Ross Sea (Antarctica) waters during austral summer 2008, *Polar Res.*, 33, 20403, doi:10.3402/polar.v33.20403, 2014.
- Robbins, L. L., Wynn, J. G., Lisle, J. T., Yates, K. K., Knorr, P. O., Byrne, R. H., Liu, X., Patsavas, M. C., Azetsu-Scott, K., and Takahashi, T.: Baseline monitoring of the western Arctic

- Ocean estimates 20 % of Canadian basin surface waters are undersaturated with respect to aragonite., *PLoS One*, 8, e73796, doi:10.1371/journal.pone.0073796, 2013.
- Roden, N. P., Shadwick, E. H., Tilbrook, B., and Trull, T. W.: Annual cycle of carbonate chemistry and decadal change in coastal Prydz Bay, East Antarctica, *Mar. Chem.*, 155, 135–147, doi:10.1016/j.marchem.2013.06.006, 2013.
- Rubin, S. I.: Carbon and nutrient cycling in the upper water column across the Polar Frontal Zone and Antarctic Circumpolar Current along 170° W, *Global Biogeochem. Cy.*, 17, 1087, doi:10.1029/2002GB001900, 2003.
- Rubin, S. I., Takahashi, T., Chipman, D. W., and Goddard, J. G.: Primary productivity and nutrient utilization ratios in the Pacific sector of the Southern Ocean based on seasonal changes in seawater chemistry, *Deep-Sea Res. Pt. I*, 45, 1211–1234, doi:10.1016/S0967-0637(98)00021-1, 1998.
- Saenz, B. T. and Arrigo, K. R.: Annual primary production in Antarctic sea ice during 2005–2006 from a sea ice state estimate, *J. Geophys. Res.-Oceans*, 119, 3645–3678, doi:10.1002/2013JC009677, 2014.
- Sandrini, S., Ait-Ameur, N., Rivaro, P., Massolo, S., Touratier, F., Tositti, L., and Goyet, C.: Anthropogenic carbon distribution in the Ross Sea, Antarctica, *Antarct. Sci.*, 19, 395–407, doi:10.1017/S0954102007000405, 2007.
- Schram, J. B., Schoenrock, K. M., McClintock, J. B., Amsler, C. D., and Angus, R. A.: Multi-frequency observations of seawater carbonate chemistry on the central coast of the western Antarctic Peninsula, *Polar Res.*, 1, 1–49, 2015.
- Seibel, B. A. and Dierssen, H. M.: Cascading Trophic Impacts of Reduced Biomass in the Ross Sea, Antarctica: Just the Tip of the Iceberg?, *Biol. Bull.*, 205, 93–97, 2003.
- Sewell, M. A. and Hofmann, G. E.: Antarctic echinoids and climate change: A major impact on the brooding forms, *Glob. Change Biol.*, 17, 734–744, doi:10.1111/j.1365-2486.2010.02288.x, 2011.
- Shadwick, E. H., Rintoul, S. R., Tilbrook, B., Williams, G. D., Young, N., Fraser, A. D., Marchant, H., Smith, J., and Tamura, T.: Glacier tongue calving reduced dense water formation and enhanced carbon uptake, *Geophys. Res. Lett.*, 40, 904–909, doi:10.1002/grl.50178, 2013.
- Shadwick, E. H., Tilbrook, B., and Williams, G. D.: Carbonate chemistry in the Mertz Polynya (East Antarctica): Biological and physical modification of dense water outflows and the export of anthropogenic CO₂, *J. Geophys. Res.-Oceans*, 119, 1–14, doi:10.1002/2013JC009286, 2014.
- Smith, W., Sedwick, P., Arrigo, K., Ainley, D., and Orsi, A.: The Ross Sea in a Sea of Change, *Oceanography*, 25, 90–103, doi:10.5670/oceanog.2012.80, 2012.
- Smith, W. O. and Gordon, L. I.: Hyperproductivity of the Ross Sea (Antarctica) polynya during austral spring, *Geophys. Res. Lett.*, 24, 233–236, doi:10.1029/96GL03926, 1997.
- Sokolov, S. and Rintoul, S. R.: Circumpolar structure and distribution of the antarctic circumpolar current fronts: 1. Mean circumpolar paths, *J. Geophys. Res.-Oceans*, 114, 1–19, doi:10.1029/2008JC005108, 2009.
- Spreen, G., Kaleschke, L., and Heygster, G.: Sea ice remote sensing using AMSR-E 89-GHz channels, *J. Geophys. Res.-Oceans*, 113, C02S03, doi:10.1029/2005JC003384, 2008.
- Stumpp, M., Hu, M. Y., Melzner, F., Gutowska, M. A., Dorey, N., Himmerkus, N., Holtmann, W. C., Dupont, S. T., Thorndyke, M. C., and Bleich, M.: Acidified seawater impacts sea urchin larvae pH regulatory systems relevant for calcification., *P. Natl. Acad. Sci. USA.*, 109, 18192–18197, doi:10.1073/pnas.1209174109, 2012.
- Suckling, C. C., Clark, M. S., Richard, J., Morley, S. A., Thorne, M. S., Harper, E. M., and Peck, L. S.: Adult acclimation to combined temperature and pH stressors significantly enhances reproductive outcomes compared to short-term exposures, *J. Anim. Ecol.*, 84, 773–784, doi:10.1111/1365-2656.12316, 2015.
- Sweeney, C.: The Annual Cycle of Surface Water CO₂ and O₂ in the Ross Sea: A model for Gas Exchange on the Continental Shelves of Antarctica, in: *Biogeochemistry of the Ross Sea*, 295–310, 2003.
- Sweeney, C., Hansell, D. A., Carlson, C. A., Codispoti, L. A., Gordon, L. I., Marra, J., Millero, F. J., Smith, W. O., and Takahashi, T.: Biogeochemical regimes, net community production and carbon export in the Ross Sea, Antarctica, *Deep-Sea Res. Pt. II*, 47, 3369–3394, doi:10.1016/S0967-0645(00)00072-2, 2000a.
- Sweeney, C., Smith, W. O., Hales, B., Bidigare, R. R., Carlson, C. A., Codispoti, L. A., Gordon, L. I., Hansell, D. A., Millero, F. J., Park, M. O., and Takahashi, T.: Nutrient and carbon removal ratios and fluxes in the Ross Sea, Antarctica, *Deep-Sea Res. Pt. II*, 47, 3395–3421, doi:10.1016/S0967-0645(00)00073-4, 2000b.
- Swift, J. H. and Orsi, A. H.: Sixty-four days of hydrography and storms: RVIB Nathaniel B. Palmer's 2011 SO4P Cruise, *Oceanography*, 25, 54–55, doi:10.5670/oceanog.2012.74, 2012.
- Tagliabue, A. and Arrigo, K. R.: Iron in the Ross Sea: 1. Impact on CO₂ fluxes via variation in phytoplankton functional group and non-Redfield stoichiometry, *J. Geophys. Res.-Oceans*, 110, 1–15, doi:10.1029/2004JC002531, 2005.
- Takahashi, T., Sutherland, S. C., Wanninkhof, R., Sweeney, C., Feely, R. A., Chipman, D. W., Hales, B., Friederich, G., Chavez, F., Sabine, C., Watson, A., Bakker, D. C. E., Schuster, U., Metzl, N., Yoshikawa-Inoue, H., Ishii, M., Midorikawa, T., Nojiri, Y., Körtzinger, A., Steinhoff, T., Hoppema, M., Olafsson, J., Arnarson, T. S., Tilbrook, B., Johannessen, T., Olsen, A., Bellerby, R., Wong, C. S., Delille, B., Bates, N. R., and de Baar, H. J. W.: Climatological mean and decadal change in surface ocean pCO₂, and net sea-air CO₂ flux over the global oceans, *Deep-Sea Res. Pt. II*, 56, 554–577, doi:10.1016/j.dsr2.2008.12.009, 2009.
- Takahashi, T., Sweeney, C., Hales, B., Chipman, D., Newberger, T., Goddard, J., Iannuzzi, R., and Sutherland, S.: The Changing Carbon Cycle in the Southern Ocean, *Oceanography*, 25, 26–37, doi:10.5670/oceanog.2012.71, 2012.
- Tortell, P. D., Payne, C. D., Li, Y., Trimborn, S., Rost, B., Smith, W. O., Riesselman, C., Dunbar, R. B., Sedwick, P., and DiTullio, G. R.: CO₂ sensitivity of Southern Ocean phytoplankton, *Geophys. Res. Lett.*, 35, L04605, doi:10.1029/2007GL032583, 2008.
- van Heuven, S., Pierrot, D., Rae, J. W. B., Lewis, E., and Wallace, D. W. R.: MATLAB program developed for CO₂ system calculations, ORNL/CDIAC-105b, Carbon Dioxide Information Analysis Center, Oak Ridge National Laboratory, US Department of Energy, Oak Ridge, TN, USA, available at: http://cdiac.ornl.gov/ftp/co2sys/CO2SYS_calc_MATLAB_v1.1/ (last access: 27 November 2015), 2011.
- Weeber, A., Swart, S., and Monteiro, P. M. S.: Seasonality of sea ice controls interannual variability of summertime Ω_A at

- the ice shelf in the Eastern Weddell Sea – an ocean acidification sensitivity study, *Biogeosciences Discuss.*, 12, 1653–1687, doi:10.5194/bgd-12-1653-2015, 2015.
- Yamamoto-Kawai, M., McLaughlin, F. A., Carmack, E. C., Nishino, S., and Shimada, K.: Aragonite undersaturation in the Arctic Ocean: effects of ocean acidification and sea ice melt, *Science*, 326, 1098–1100, doi:10.1126/science.1174190, 2009.
- Yu, P. C., Sewell, M. A., Matson, P. G., Rivest, E. B., Kapsenberg, L., and Hofmann, G. E.: Growth attenuation with developmental schedule progression in embryos and early larvae of *Sterechinus neumayeri* raised under elevated CO₂, *PLoS One*, 8, e52448, doi:10.1371/journal.pone.0052448, 2013.